

TRANSITIONAL CORES AND FUEL CYCLE ANALYSES IN SUPPORT OF MIT REACTOR LOW ENRICHED URANIUM FUEL CONVERSION

Kaichao Sun*, Akshay Dave, and Lin-wen Hu

kaichao@mit.edu

*Nuclear Reactor Laboratory, Massachusetts Institute of Technology
138 Albany St., Cambridge, MA 02139, USA*

Erik Wilson, Thad Heltemes, Son Pham, and David Jaluvka

*Nuclear Engineering Division, Argonne National Laboratory
9700 S. Cass Ave., Argonne, IL 60439, USA*

ABSTRACT

The Massachusetts Institute of Technology Reactor (MITR) is a research reactor in Cambridge, Massachusetts designed primarily for experiments using neutron beam and in-core irradiation facilities. At 6 MW, it delivers neutron flux and energy spectrum comparable to power light water reactors (LWRs) in a compact core using highly enriched uranium (HEU) fuel. In the framework of non-proliferation policy, research and test reactors have started a program to convert HEU fuel to low enriched uranium (LEU) fuel. A new type of LEU fuel based on a high density alloy of uranium and molybdenum (U-10Mo) is expected to allow conversion of U.S. high performance research reactors (USHRRs) like the MITR. The principal part of the Preliminary Safety Analysis Report (PSAR) has been completed for the MITR LEU conversion. A transition core plan, from 22 fresh LEU fuel elements (i.e., beginning-of-life) gradually to 24 of them arranged in an equilibrium configuration, is expected to serve as an appendix chapter in the PSAR. The current study presents the fuel cycle development, which eventually leads to the transition core plan. The results confirm the equilibrium state, where both the shim bank movement (i.e., core reactivity) as well as the content of fissile materials stabilize, can be achieved by fixed-pattern fuel management. Fission density has been evaluated for a number of fully discharged LEU fuel elements, using both conservative and best-estimate approaches. There are adequate margins to the planned qualification fission density limit of three different MITR U-10Mo plate configurations. The fuel cycle calculations also generate power profiles at each core state. A steady-state thermal-hydraulic safety analysis has thus been performed, where onset of nucleate boiling (ONB) is considered as the safety criterion. The results confirm significant margins to ONB at all analyzed transition and equilibrium fuel cycle states.

1. Introduction

The Massachusetts Institute of Technology Reactor (MITR) is a research reactor designed primarily for experiments using neutron beams and in-core irradiation facilities. The original

version, MITR-I, was a heavy-water moderated and cooled nuclear research reactor. After a reevaluation of the utilization needs and further core optimization studies, it underwent a major upgrade and the current reactor design, MITR-II, began operation in 1976. The reactor is moderated and cooled by light water and has a heavy-water reflector. The thermal power of the MITR was updated from 5 MW to 6 MW in 2011 in conjunction with the 20-year license renewal [1].

The MITR uses rhomboid-shaped fuel elements. The 27 in-core positions for fuel elements and/or irradiation experiments are illustrated in Figure 1. These positions are divided into three concentric rings – the inner ring with three, the middle ring with nine, and the outer ring with 15 rhomboid-shaped areas. The edge-to-edge distances of the three concentric hexagons of the fuel region are 12.4 cm, 25.5 cm, and 38.4 cm, respectively. Each fuel element contains 15 fuel plates, which consist of ~ 93% highly enriched uranium (HEU) sandwiched between sides of aluminum cladding. The surrounding core tank has a cylindrical shape, 52 cm in diameter and 73 cm in height. There is a heavy-water reflector surrounding the reactor core from the sides and the bottom. In addition, a three-meter high light-water plenum sits above the core tank, providing effective neutron shielding.

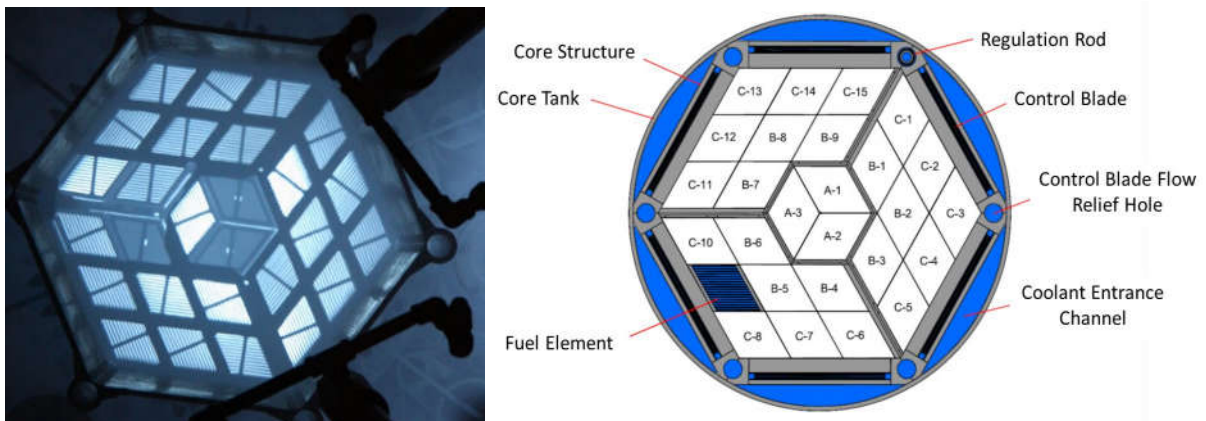


Fig. 1. Top view of the MITR core (left) and horizontal cross-section (right).

In the framework of non-proliferation policy, the MITR is planning to convert from HEU to low enriched uranium (LEU) fuel. A new type of LEU fuel based on a high-density alloy of uranium and molybdenum is expected to allow the conversion of all U.S. high performance reactors (USHPRRs) including the MITR [2]. Previous research efforts have been made for a specific 19-plate fuel element design, known as 19B25 [3]. The impact on beam applications and in-core experiment program due to the conversion has also been investigated [4]. The Preliminary Safety Analysis Report (PSAR) for the MITR LEU conversion has been submitted to the

U.S. Nuclear Regulatory Commission (NRC) in December 2017 [5]. A transition core plan, from 22 fresh LEU fuel elements (i.e., beginning-of-life) gradually to a 24-element equilibrium core configuration, becomes necessary to ensure all core parameters can be maintained within the safety envelope during conversion. This paper summarizes the fuel cycle development work supporting such a transition core plan.

2. Methods

2.1. MITR LEU Fuel Element Design

Efforts have been made to design an MITR LEU fuel element with the same outer dimensions that could safely replace the current MITR HEU fuel element and maintain core performance while requiring minimal, if any, changes to the reactor system. Designs of the LEU plate-type fuel elements have retained the same rhomboid-shape outer dimensions. After extensive fuel development and qualification efforts, high-density U-10Mo monolithic alloy has been selected for the MITR LEU fuel [6]. The U-235 enrichment is 19.75 %, with a fuel density of 15.3 g-U/cm³.

One of the LEU elements was designed with 18 thinner plates (recommended from a thermal-hydraulic viewpoint) with 0.51 mm (20 mils) thick fuel and 0.25 mm (10 mils) cladding thickness and the same longitudinal fins as the HEU element. Recent fuel development experience has led to a re-evaluation of the minimum cladding thickness to enhance fuel fabricability. These fuel core and fuel element design activities were undertaken to determine if additional cladding thickness could be incorporated into an MITR LEU element design. Since increased cladding thickness would displace water and degrade core reactivity, removal of the fins was proposed. Removal of the fins would not only increase water to metal ratio in the core, but would also reduce the cost of the MITR LEU element by eliminating this fabrication step, which is unique to the MITR among all USHPRRs. In order to compensate for the loss of a heat transfer area, an increased core coolant flow rate has been considered, and reduced fuel thicknesses were introduced in the outer plates of each element to limit heat flux peaking. One final candidate, known as 19B25, was down-selected from a number of potential LEU fuel designs. It consists of 19 LEU fuel plates. Each fuel plate has a nominal total thickness of 1.24 mm (49 mils). The nominal/standard plate design has fuel meat thickness of 0.64 mm (25 mils) and un-finned cladding thickness of 0.30 mm (12 mils). The code “B” represents the fuel meat thickness reduction for the first three outer plates from each end plate (i.e., Plate No. 1 and 19) by 48 %, 32 %, and 32 %, respectively. The engineering drawing is shown in Figure 2 and detailed information can be found in [3]. A comparison of the HEU and LEU (finned and un-finned 19B25) fuel design parameters is shown in Table I. The 19B25 design is now the baseline design.

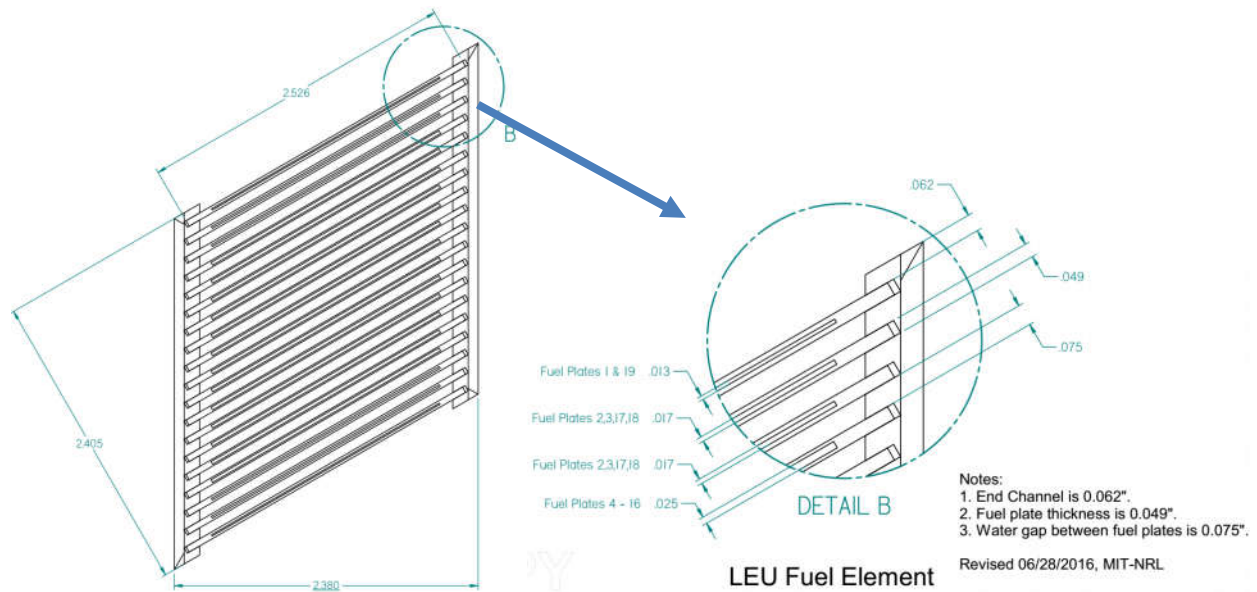


Fig. 2. Engineering drawing of MITR LEU fuel design.

Table I. Comparison of current HEU and proposed LEU fuel designs

| | HEU Finned (UAl _x) | LEU Finned (U-Mo) | LEU 19B25 (U-Mo) |
|-------------------------------------|--------------------------------------|-------------------------|------------------------|
| U-235 Enrichment (%) | 93.15 | 19.75 | 19.75 |
| U-235 per Element (g) | 508 | 931 | 968 |
| Fuel Density (g-U/cm ³) | 1.54 | 15.5 | 15.5 |
| Plates per Element | 15 | 18 | 19 |
| Plate Thickness (mm) | 1.52 | 1.02 | 1.24 |
| Fins on Cladding | Yes | Yes | No |
| Operating Power (MW) | 6.0 | 7.0 | 7.0 |
| Nominal Flow Rate (gpm) | 2000 | 2400 | 2400 |
| Cycle Length (days) | 40-50 | 55-70 | 55-70 |

2.2. Fission Density Limit

As indicated in the previous subsection and listed in Table II below, there are three different MITR LEU fuel plate configurations: 1) F-Plate, 2) Y-Plate, and 3) T-Plate. These plates feature the same outer dimensions. Their combinations of fuel core and cladding thickness are, however, different.

The research reactor fuel discharge criterion is primarily based on the maximum allowed fission density (i.e., fission events per unit volume). Each MITR LEU fuel plate configuration corresponds to a specific fission density limit [5]. The limiting values are listed in Table II.

Table II. Fission density limit of three different fuel plate configurations

| | F-Plate | Y-Plate | T-Plate |
|--|----------------------|----------------------|----------------------|
| Plate Number | 4 – 16 | 2, 3, 17, 18 | 1, 19 |
| Fuel thickness (mm) | 0.64 | 0.43 | 0.33 |
| Clad thickness (mm) | 0.30 | 0.41 | 0.46 |
| Fission density limit (fission/cm ³) | 3.6×10^{21} | 4.4×10^{21} | 5.0×10^{21} |

2.3. Thermal-Hydraulic Limit

Onset of nucleate boiling (ONB) is adopted for the steady-state thermal-hydraulics limit. When the energy flux to a heated surface is increased slowly, the first two-phase behavior that is observed is ONB, also called incipient boiling. It defines the conditions where bubbles first start to form on the heated surface. Because most of the liquid is still subcooled, the bubbles do not detach but grow and collapse while attached to the wall. ONB is followed by onset of significant voiding (OSV), which describes the condition where the bubbles grow larger on the heated surface and detach regularly. OSV leads to onset of flow instability (OFI), which describes the condition when the mass flow rate decreases with increasing vapor content in the coolant flow. This type of flow excursion will lead to an elevated fuel temperature, because of an abrupt drop in the coolant flow rate. Experimental studies have shown that OFI tends to occur closely after OSV, when the increase in vapor content results in a higher friction pressure drop [7]. Eventually, critical heat flux (CHF) denotes the condition at which the heat transfer of two-phase flow deteriorates substantially and subsequently leads to elevated fuel temperatures. CHF may occur, because of either vapor film formation on the clad surface or dryout of the liquid film. Because the rise in temperature quickly follows CHF, it is desirable to use some phenomenon, one that occurs at the earliest stage, as the basis for the steady-state thermal-hydraulics safety.

For the steady-state MITR operation, ONB is adopted as the safety criterion for limiting safety system settings (LSSS) [1]. Sudo et al. suggested the Bergles-Rohsenow correlation for the prediction of ONB for narrow rectangular coolant channels [8]. This suggestion was based on comparisons of several existing correlations with experimental data. Sudo et al. also concluded that the Bergles-Rohsenow correlation predicts the lower limits of the measured ONB temperatures for given heat fluxes and that there exists a margin between the predicted and measured ONB temperatures. The Bergles-Rohsenow correlation predicts the fuel clad

temperature at which ONB occurs (see Eq. 1). It should be noted that this correlation is applicable to both forced convection and natural circulation.

$$T_{\text{clad,ONB}} = T_{\text{sat}} + 0.556 \cdot \left[\frac{q''}{1082 \cdot p^{1.156}} \right]^{0.463 \cdot p^{0.0234}} \quad \text{Eq. 1}$$

where $T_{\text{clad,ONB}}$ is the fuel clad temperature ($^{\circ}\text{C}$) at which ONB occurs, T_{sat} is the saturation temperature ($^{\circ}\text{C}$), q'' is the local heat flux (W/m^2), and p is the pressure (bar).

2.4. Computational Tools

The neutronics calculations, including the fuel cycle simulations, are performed using the in-house depletion code MCODE (MCNP-ORIGEN Coupled Depletion Program) [9]. The main workhorse of this code package consists of the general purpose Monte Carlo transport code MCNP5_v1.60 [10] and the point-depletion code ORIGEN-2.2 [11]. The former provides snapshot physics results of the studied system, in particular the continuous-energy neutron flux distribution of the entire MITR core model. The one-group macroscopic cross-section is generated by weighting the point-wise microscopic cross-section (included in nuclear and atomic data libraries) with the energy-dependent neutron flux. MCODE is the external link to transfer the macroscopic cross-sections of all the involved isotopes to ORIGEN. The latter adopts the matrix exponential method to solve a large system of coupled linear first-order ordinary differential equations with constant coefficients. The material compositions can be, therefore, updated by taking into account neutron absorption and radioactive decay within a pre-defined time frame. MCODE then sends back the updated material compositions to MCNP and initiates a new round of a neutron transport calculation. It should be noted that MCODE adopts a predictor-corrector method to calculate nuclide concentrations for each time-step, which has been shown to be more accurate than the methods used in other similar codes that adopt only the beginning-of-step or middle-of-step reaction rates for the depletion matrix in the Bateman equations [9].

A Python wrapper code MCODE-FM [12, 13], is specifically designed for MITR fuel management as the extension of MCODE. (FM stands for Fuel Management.) It contains all geometry information of the MITR core and enables the rhomboid-shaped MITR fuel elements to be rotated and flipped. A criticality search algorithm to track the critical blade movement has been implemented. In addition, MCODE-FM features an automation of input file generation, data manipulation, and post-processing of the output data for fuel cycle analysis. The code package associated with the MITR depletion model has been extensively validated against experimental data, including historical start-up cores, fission product poisoning and fuel depletion reactivity effects, reaction rate based thermal and fast neutron flux, and etc. [2, 14].

In the depletion model, the discretization of the material zones can be made in axial, radial (i.e., grouping of fuel plates), and lateral (i.e., dividing fuel plate into stripes) directions. The present study adopts 16 uniform axial nodes for each of the MITR LEU fuel elements. Each element's 19 fuel plates are divided into ten groups, with plate numbers of 1/2/3/4/5-9/10-15/16/17/18/19, respectively. The uneven radial grouping is introduced in order to model the enhanced moderation more accurately at the core periphery. According to [15], power peaking occurs at the end plate, when the fuel element is facing the outside of the reactor core. The fuel plates are further sub-divided into four uniform lateral nodes. Overall, the currently adopted discretization scheme is sufficient and it adequately computes most of the flux/depletion gradients in the MITR core.

For thermal-hydraulic analyses the system code RELAP5 [16], and the proprietary code STAT7 [17], are used. The Argonne National Laboratory (ANL) is the developer of STAT7. The STAT7 code was written to automate the thermal hydraulic safety calculations for the MITR, for conversion to LEU fuel and for future fuel re-loads after the conversion. A Monte-Carlo statistical propagation approach is used to treat uncertainties in important parameters in the analysis. STAT7 is only capable of providing steady-state analyses. However, due to its focused purpose, calculations involving over 104 histories take several minutes to run, employing a single processor thread on a modern computer. The nominal output from STAT7 was verified against RELAP5, as discussed in Section 3.3. The fuel element is divided in a number of lateral stripes (quarter element slices), as presented in Figure 5. This geometry is intended to capture the temperature peak at the sides of the MITR fuel element.

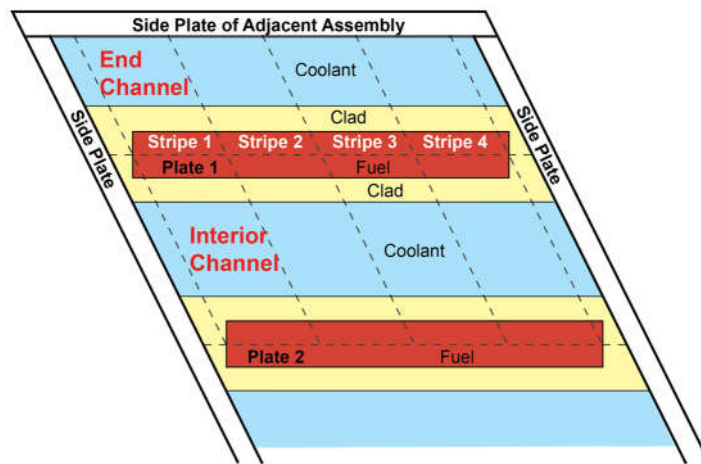


Fig. 5: STAT7 channel geometry for four stripes.

2.5. Statistical Analysis using STAT7

In the statistical analyses of the LEU transition cores performed with STAT7, several statistical parameters were established to quantify the safety margin. The established 3-sigma statistical parameters are presented in Table III.

The statistical settings used by STAT7 are presented in Table IV. In a STAT7 run, the desired ONB probability is set a priori (0.135% in the current analyses). In the initial calculation, the nominal power and mass flow rate is used and 4000 samples are generated for each batch using the statistical parameters. The number of cases at which ONB is reached is tallied. If the probability of ONB occurring is less than 0.135%, the nominal reactor power is increased. The power is iterated upon until the desired ONB probability is reached, within a certain tolerance level.

Table III. Statistical parameters used in calculations

| Parameter | 3 σ [%] |
|--|----------------|
| Reactor power measurement uncertainty | 5 |
| Local power density measurement/calculation and fuel homogeneity | 15.56 |
| Pump flow measurement uncertainty | 5 |
| Nominal coolant channel/gap uncertainty | 5.63 |
| Heat transfer coefficient uncertainty | 20 |

Table IV. STAT7 settings for statistical analysis

| STAT7 Settings | Value |
|-------------------|--------|
| Number of batches | 25 |
| Number of samples | 4000 |
| ONB probability | 0.135% |

2.6. Transition Core Plan

The PSAR for the MITR LEU conversion is near its completion. A transition core plan, from 22 fresh LEU elements (i.e., beginning-of-life) gradually to a 24-element equilibrium core configuration, is also expected by the U.S. Nuclear Regulatory Commission (NRC) as an

appendix in the PSAR. The goal is to ensure all core parameters can be maintained within the safety envelope during the entire conversion process. The primary focus of the current analysis is to develop such a transition core plan.

The current MITR fuel management scheme is largely based on empirical decisions. Even though state-of-the-art computational tools serve as a solid technical basis, the refueling plan is still largely based on human intervention. This is, on the one hand, a considerable burden. On the other hand, higher probability of human errors is anticipated, when the planning process relies on empirical decisions. Given the robust LEU fuel system, which generally allows deeper burnup due to a significantly increased fission density limit, the MITR fuel cycle will no longer be limited by the discharge burnup, but rather the core criticality (i.e., sufficient fissile materials to maintain the nuclear chain reactions). A fixed refueling pattern, which may not optimize the spatial depletion to full extent, becomes more justifiable. Furthermore, an equilibrium fuel cycle state can be expected after applying multiple routine fuel management operations based on fixed refueling pattern. The pattern is proposed as follows and is illustrated in Figure 3:

- 1) All fuel elements stay in their own $\frac{1}{3}$ of the core for entire lifetime. (Indicated with different colors)
- 2) Fresh fuel elements will be added into B-ring and stay there for three cycles. (Exceptions for A-2 Position¹)
- 3) The three-cycle-old B-ring elements will be flipped and reshuffled to C-ring positions.
- 4) The flipped and reshuffled elements will stay in C-ring for five more cycles.
- 5) C-ring elements will be rotated once before their 4th (or 2nd last) C-ring cycle.
- 6) Five-cycle-old C-ring elements will be discharged.

¹ It is typically not recommended to load fresh elements to the A-ring positions, since the power peaks may occur in these positions due to geometrical buckling.

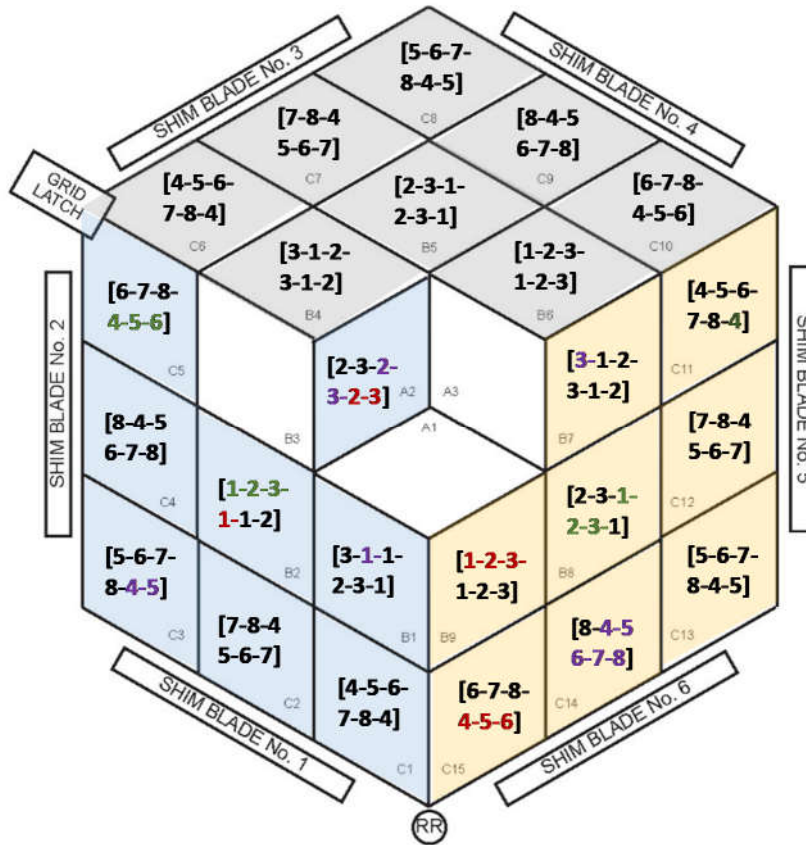


Fig. 3. Fixed pattern for MITR LEU fuel management².

Figure 4 shows an element-by-element path towards equilibrium fuel cycle, where total of 60 MITR LEU fuel elements are involved in the process. The first seven cycles are considered as a transition period. The following seven cycles are equilibrium cycles.

² The numbers within the square brackets indicate cycle index for fuel element at each in-core position, e.g., “1” represents loading of a fresh element. At “4”, the element will be shuffled to a C-ring position. “8” is the last cycle of each element. The different colors of the numbers intend to illustrate the path of several fuel elements.

| Cycle | 1 | 2 | 3 | 4 | 5 | 6 | 7 | 8 | 9 | 10 | 11 | 12 | 13 | 14 |
|--------|------|---------|--------|--------|--------|--------|--------|--------|--------|--------|--------|--------|--------|--------|
| Weeks | 10+3 | 10+3 | 10+3 | 10+3 | 10+3 | 10+3 | 10+3 | 10+3 | 10+3 | 10+3 | 10+3 | 10+3 | 10+3 | 10+3 |
| ML-101 | A2 | A2 | f: C3 | C3 | C3 | r: C3 | C3 | DIS | DIS | DIS | DIS | DIS | DIS | DIS |
| ML-102 | B1 | B1 | B1 | f: C1 | C1 | C1 | r: C1 | C1 | DIS | DIS | DIS | DIS | DIS | DIS |
| ML-103 | B2 | B2 | A2 | A2 | f: C4 | C4 | C4 | r: C4 | C4 | DIS | DIS | DIS | DIS | DIS |
| ML-104 | B4 | B4 | f: C8 | C8 | C8 | r: C8 | C8 | DIS | DIS | DIS | DIS | DIS | DIS | DIS |
| ML-105 | B5 | B5 | B5 | f: C6 | C6 | C6 | r: C6 | C6 | DIS | DIS | DIS | DIS | DIS | DIS |
| ML-106 | B7 | B7 | f: C13 | C13 | C13 | r: C13 | C13 | DIS | DIS | DIS | DIS | DIS | DIS | DIS |
| ML-107 | B8 | B8 | B8 | f: C11 | C11 | C11 | r: C11 | C11 | DIS | DIS | DIS | DIS | DIS | DIS |
| ML-108 | C1 | r: C1 | C1 | WS | WS | WS | WS | WS | WS | WS | WS | WS | WS | WS |
| ML-109 | C2 | C2 | C2 | r: C2 | C2 | WS | WS | WS | WS | WS | WS | WS | WS | WS |
| ML-110 | C3 | C3 | WS | WS | WS | WS | WS | WS | WS | WS | WS | WS | WS | WS |
| ML-111 | C4 | C4 | r: C4 | C4 | WS | WS | WS | WS | WS | WS | WS | WS | WS | WS |
| ML-112 | C5 | C5 | C5 | C5 | r: C5 | C5 | WS | WS | WS | WS | WS | WS | WS | WS |
| ML-113 | C6 | r1: C6 | C6 | WS | WS | WS | WS | WS | WS | WS | WS | WS | WS | WS |
| ML-114 | C7 | C7 | C7 | r: C7 | C7 | WS | WS | WS | WS | WS | WS | WS | WS | WS |
| ML-115 | C8 | C8 | WS | WS | WS | WS | WS | WS | WS | WS | WS | WS | WS | WS |
| ML-116 | C9 | C9 | r: C9 | C9 | WS | WS | WS | WS | WS | WS | WS | WS | WS | WS |
| ML-117 | C10 | C10 | C10 | C10 | r: C10 | C10 | WS | WS | WS | WS | WS | WS | WS | WS |
| ML-118 | C11 | r1: C11 | C11 | WS | WS | WS | WS | WS | WS | WS | WS | WS | WS | WS |
| ML-119 | C12 | C12 | C12 | r: C12 | C12 | WS | WS | WS | WS | WS | WS | WS | WS | WS |
| ML-120 | C13 | C13 | WS | WS | WS | WS | WS | WS | WS | WS | WS | WS | WS | WS |
| ML-121 | C14 | C14 | r: C14 | C14 | WS | WS | WS | WS | WS | WS | WS | WS | WS | WS |
| ML-122 | C15 | C15 | C15 | C15 | r: C15 | C15 | WS | WS | WS | WS | WS | WS | WS | WS |
| ML-123 | - | B6 | B6 | B6 | f: C9 | C9 | C9 | r: C9 | C9 | DIS | DIS | DIS | DIS | DIS |
| ML-124 | - | - | B9 | B9 | f: C14 | C14 | C14 | r: C14 | C14 | DIS | DIS | DIS | DIS | DIS |
| ML-125 | - | - | B2 | B2 | B2 | f: C2 | C2 | C2 | r: C2 | C2 | DIS | DIS | DIS | DIS |
| ML-126 | - | - | B4 | B4 | B4 | f: C7 | C7 | C7 | r: C7 | C7 | DIS | DIS | DIS | DIS |
| ML-127 | - | - | B7 | B7 | B7 | f: C12 | C12 | C12 | r: C12 | C12 | DIS | DIS | DIS | DIS |
| ML-128 | - | - | - | - | A2 | A2 | f: C5 | C5 | C5 | r: C5 | C5 | DIS | DIS | DIS |
| ML-129 | - | - | - | B5 | B5 | B5 | f: C10 | C10 | C10 | r: C10 | C10 | DIS | DIS | DIS |
| ML-130 | - | - | - | B8 | B8 | B8 | f: C15 | C15 | C15 | r: C15 | C15 | DIS | DIS | DIS |
| ML-131 | - | - | - | - | B1 | B1 | B1 | f: C3 | C3 | C3 | r: C3 | C3 | DIS | DIS |
| ML-132 | - | - | - | - | B6 | B6 | B6 | f: C8 | C8 | C8 | r: C8 | C8 | DIS | DIS |
| ML-133 | - | - | - | - | B9 | B9 | B9 | f: C13 | C13 | C13 | r: C13 | C13 | DIS | DIS |
| ML-134 | - | - | - | - | - | B2 | A2 | A2 | f: C1 | C1 | C1 | r: C1 | C1 | DIS |
| ML-135 | - | - | - | - | - | B4 | B4 | B4 | f: C6 | C6 | C6 | r: C6 | C6 | DIS |
| ML-136 | - | - | - | - | - | B7 | B7 | B7 | f: C11 | C11 | C11 | r: C11 | C11 | DIS |
| ML-137 | - | - | - | - | - | - | B2 | B2 | B2 | f: C4 | C4 | C4 | r: C4 | C4 |
| ML-138 | - | - | - | - | - | - | B5 | B5 | B5 | f: C9 | C9 | C9 | r: C9 | C9 |
| ML-139 | - | - | - | - | - | - | B8 | B8 | B8 | f: C14 | C14 | C14 | r: C14 | C14 |
| ML-140 | - | - | - | - | - | - | - | B1 | A2 | A2 | f: C2 | C2 | C2 | r: C2 |
| ML-141 | - | - | - | - | - | - | - | B6 | B6 | B6 | f: C7 | C7 | C7 | r: C7 |
| ML-142 | - | - | - | - | - | - | - | B9 | B9 | B9 | f: C12 | C12 | C12 | r: C12 |
| ML-143 | - | - | - | - | - | - | - | - | B1 | B1 | B1 | f: C5 | C5 | C5 |
| ML-144 | - | - | - | - | - | - | - | - | B4 | B4 | B4 | f: C10 | C10 | C10 |
| ML-145 | - | - | - | - | - | - | - | - | B7 | B7 | B7 | f: C15 | C15 | C15 |
| ML-146 | - | - | - | - | - | - | - | - | - | B2 | A2 | A2 | f: C3 | C3 |
| ML-147 | - | - | - | - | - | - | - | - | - | B5 | B5 | B5 | f: C8 | C8 |
| ML-148 | - | - | - | - | - | - | - | - | - | B8 | B8 | B8 | f: C13 | C13 |
| ML-149 | - | - | - | - | - | - | - | - | - | B2 | B2 | B2 | f: C1 | C1 |
| ML-150 | - | - | - | - | - | - | - | - | - | B6 | B6 | B6 | f: C6 | C6 |
| ML-151 | - | - | - | - | - | - | - | - | - | B9 | B9 | B9 | f: C11 | C11 |
| ML-152 | - | - | - | - | - | - | - | - | - | - | B1 | A2 | A2 | A2 |
| ML-153 | - | - | - | - | - | - | - | - | - | - | B4 | B4 | B4 | B4 |
| ML-154 | - | - | - | - | - | - | - | - | - | - | B7 | B7 | B7 | B7 |
| ML-155 | - | - | - | - | - | - | - | - | - | - | - | - | B1 | B1 |
| ML-156 | - | - | - | - | - | - | - | - | - | - | - | - | B5 | B5 |
| ML-157 | - | - | - | - | - | - | - | - | - | - | - | - | B8 | B8 |
| ML-158 | - | - | - | - | - | - | - | - | - | - | - | - | - | B2 |
| ML-159 | - | - | - | - | - | - | - | - | - | - | - | - | - | B6 |
| ML-160 | - | - | - | - | - | - | - | - | - | - | - | - | - | B9 |

Fig. 4. Element-by-element path towards equilibrium fuel cycle of the MITR LEU core
ML: MIT-LEU Fuel Docket Number, f: Flip, r: Rotate, WS: Wet Storage, DIS: Discharge

In the transition period, the first cycle will be loaded with 22 fresh fuel elements and one more element will be added in the following cycle. There will be four fresh fuel elements added in the third cycle, while three partially depleted fuel elements will be moved to the Wet Storage (WS) ring as long-term backup. From the fourth to the seventh cycle, there will be constantly three fresh elements in and three partially depleted elements out (as a backup). During the entire transition period (i.e., first seven cycles), 39 fresh elements are loaded and 15 partially depleted ones are stored as backup fuel. Starting from Cycle 8, three fresh fuel elements are loaded in and three fully depleted fuel elements are discharged from the reactor core at the beginning of each cycle. As a result, 21 fresh elements are loaded and 21 fully depleted elements are discharged between equilibrium Cycles 8 and 14. It should be mentioned that a 10-week power run (at 7 MW) and a 3-week decay time are modeled for each cycle.

3. Results

3.1. Transition and Equilibrium Fuel Cycles

As indicated in the previous section, the fuel cycle computational tool MCODE-FM employs a criticality search algorithm to track critical shim bank positions during reactor operation. In the current analysis, four depletion steps within each power cycle are selected: 0 days (i.e., beginning of cycle – BOC), 3 days (i.e., xenon equilibrium condition, also referred as middle of cycle – MOC), 40 days, and 70 days (or 10 weeks; i.e., end of cycle – EOC). The decay time between power cycles is 21 days (or 3 weeks). The shim bank movement results and evolutions of the total mass of major fissile isotopes (U-235 and Pu-239) in the reactor core are shown in Figures 6 and 7, respectively.

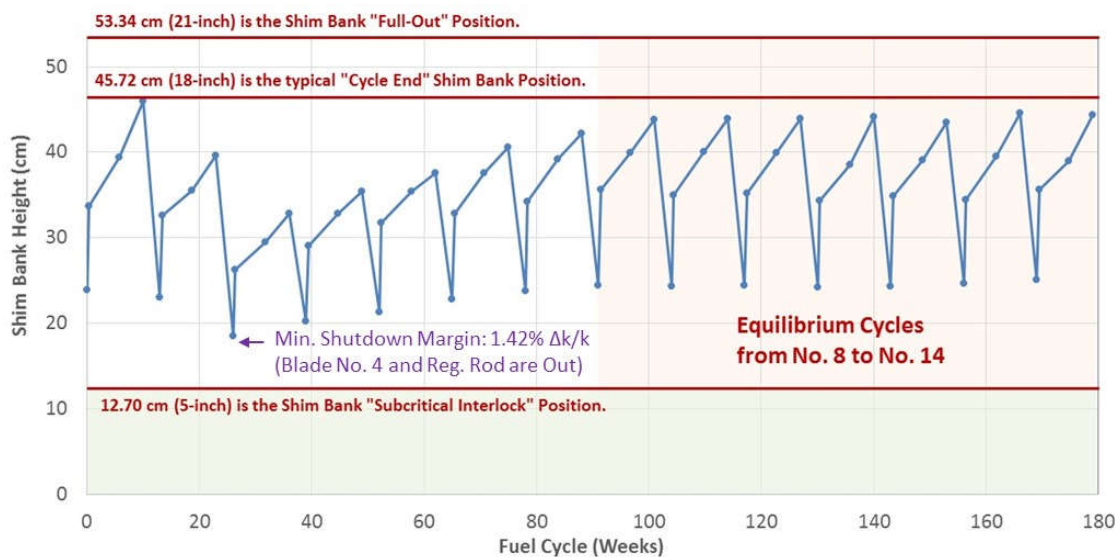


Fig. 6. Shim bank movement during transition and equilibrium fuel cycles.

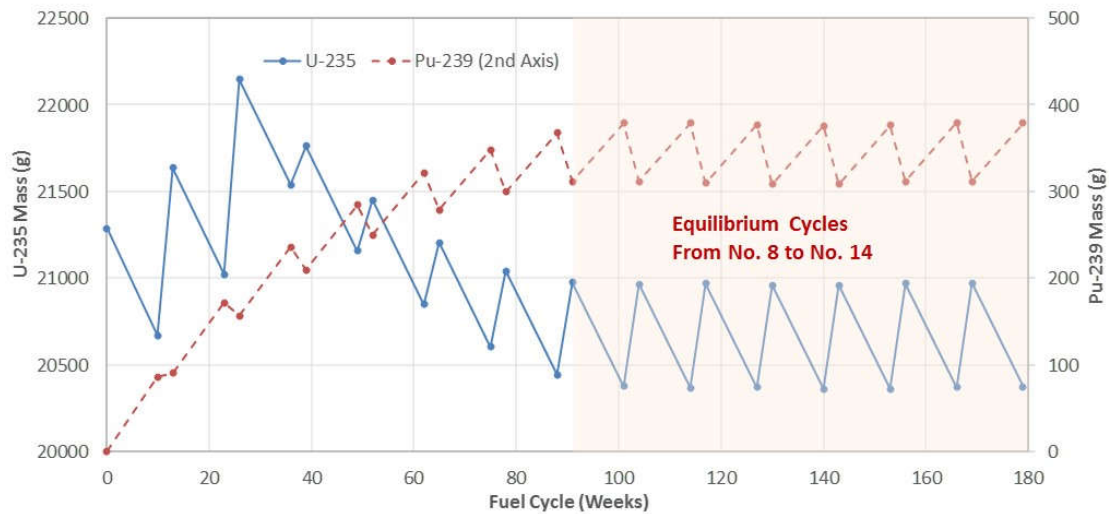


Fig. 7. U-235 and Pu-239 mass evolutions during transition and equilibrium fuel cycles.

One can see that the shim bank will be typically raised up by 10 cm during the first three days of each power cycle. This is the time period when xenon reaches equilibrium. Thereafter, the shim bank will be kept raising in a moderate slope for the rest of the cycle. This corresponds to the rate of fuel depletion. The restoration of the shim bank after each power cycle (10 weeks) is due to the combined effect of the xenon decay (3 weeks) and refueling.

Throughout the studied 14 fuel cycles, the BOC shim bank heights are always above the so-called “Subcritical Interlock” position (12.70 cm or 5.0 in) with appropriate margins and the EOC values are always kept below the typical “Cycle End” position (45.72 cm or 18 in) to maintain the capability of overcoming the xenon peak reactivity. The results of the analysis indicate that the LEU fuel offers the potential of a longer fuel cycle than 10 weeks. However, the 10 + 3 (i.e., power weeks + decay weeks) combination perfectly supports the quarterly fuel cycle strategy, which is considered optimal for our reactor experiment program.

The global shim bank movement can be largely explained by the U-235 total mass evolution in the studied fuel cycles. The initial descent (for the first three cycles) is due to the transition from the 22-element to the 24-element core. The subsequent ascent (for the following five cycles) is caused by storing partially depleted fuel elements in the WS ring rather than by discharging fully burned ones. The equilibrium state is reached beginning from the eighth cycle, which features a stabilized shim bank movement as well as U-235 and Pu-239 total mass evolution in each cycle. The average U-235 burnup is 21% (or ~ 200 g) in the discharged LEU fuel element, comparing to 37% (or ~ 190 g) for

the current HEU fuel. The average Pu-239 buildup is ~ 24 g in the discharged LEU fuel element, comparing to ~ 0.9 g for the current HEU fuel.

3.2. Fission Density Evaluation

Fission density has been tracked for six LEU fuel elements (ML-134, -135, -136, -137, -138, and -139) using a best-estimated approach, where all the fuel management actions (i.e., reshuffling, flipping, and rotation) have been taken into account. The fission density calculation relies on the F7 tally in MCNP5 (i.e., track length estimate of fission energy deposition). The tallied values at different states (i.e., BOC, MOC, and EOC) are normalized to the 7-MW core power and integrated over their depletion time of each fuel cycle. The detailed method for calculating fission density is described in [18]. The lifetime results of the peak burn-up node in the analyzed elements are summarized in Table III. As seen, significant margins to the limit values are kept for all plate types.

The best-estimated results in Table V confirm an earlier statement in Section 2.6: The MITR fuel cycle will no longer be limited by the discharge burnup, but rather by the core criticality. For further assurance, a conservative approach is also adopted. The maximum heat flux in equilibrium cycles for a calculation node (i.e., fuel plate area $1/16$ in height and $1/4$ in width) is 53.6 W/cm^2 . This indicates a maximum node fission power of 503.5 W for a fission density calculation. Such a peak value is then applied to a calculation node for its lifetime of eight fuel cycles (i.e., 560 full power days). This is an extremely conservative assumption, which leads to the overall fission energy release of 24.36 MJ. The resulting fission densities are 2.53×10^{21} , 3.72×10^{21} , and 4.86×10^{21} fission/cm³ for F-Plate, Y-Plate, and T-Plate, respectively. These values are still well bounded by the developed U-10Mo fuel fission density limits with comfortable margins.

Table V. Peak fission density (fission/cm³) values of six LEU fuel elements using best-estimate approach

| Fuel Doc. Number | F-Plate | Y-Plate | T-Plate |
|------------------|---|---|---|
| ML-134 | 1.84×10^{21} | 2.38×10^{21} | 2.82×10^{21} |
| ML-135 | 1.88×10^{21} | 2.49×10^{21} | 2.97×10^{21} |
| ML-136 | 1.97×10^{21} | 2.57×10^{21} | 3.04×10^{21} |
| ML-137 | 1.94×10^{21} | 2.29×10^{21} | 2.50×10^{21} |
| ML-138 | 1.92×10^{21} | 2.24×10^{21} | 2.46×10^{21} |
| ML-139 | 1.87×10^{21} | 2.21×10^{21} | 2.41×10^{21} |
| Limit | 3.6×10^{21} | 4.4×10^{21} | 5.0×10^{21} |

3.3. STAT7-RELAP5 Code-to-Code Comparison

In order to verify the STAT7 output, initial efforts were focused on the comparison with an equivalent stripe-geometry model implemented in RELAP5. A comparison of the cladding outer temperature is presented in Figure 8 (similar verifications have been made for the fuel centerline and bulk coolant temperatures). Both codes have good agreement (within 0.1%) in predicted “node center” temperatures, where the values are averaged within one computational node, for all transition cycles and states considered.

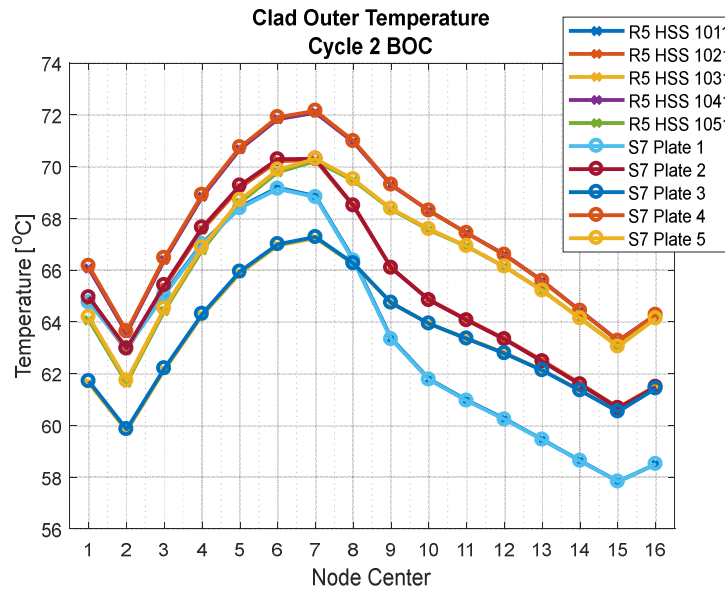


Fig. 8. STAT7-RELAP5 (S7-R5) code-to-code comparison for cladding outer temperature prediction.

3.4. Statistical Analysis for Max. LSSS Power

The LSSS power level for each cycle-state was determined using STAT7. Results for the BOC and EOC states are presented in Table VI for all 14 cycles. It should be noted that in the LSSS operation, the total core mass flow rate is reduced from 151 kg/s to 138 kg/s, and the nominal power level is increased from 7 MW to 8.7 MW. The converged power level is determined by STAT7 using parameters and settings discussed in Section II.E. The STAT7-predicted power levels are sufficiently higher than the LSSS value. The lowest margin for BOC occurs for cycle five at 9.06 MW. The location at which ONB occurs most for this cycle state is plate 16 and axial node 10 (total of 16 nodes are used).

Table VI. STAT7 statistical output for operation at LSSS. The converged power level (P), and location at which ONB occurs most (Plt. And Node) is tabulated

| Cycle | BOC | | | | | EOC | | | | |
|-------|----------|-------------------------|----------------|------|------|----------|-------------------------|----------------|------|------|
| | P [MW] | ε_{ONB} [%] | σ_{ONB} | Plt. | Node | P [MW] | ε_{ONB} [%] | σ_{ONB} | Plt. | Node |
| 1 | 9.96 | 0.134 | 0.011 | 16 | 10 | 9.52 | 0.135 | 0.014 | 1 | 10 |
| 2 | 9.74 | 0.136 | 0.010 | 16 | 11 | 9.65 | 0.135 | 0.012 | 4 | 9 |
| 3 | 9.08 | 0.137 | 0.012 | 16 | 10 | 10.03 | 0.138 | 0.011 | 16 | 10 |
| 4 | 9.60 | 0.133 | 0.010 | 16 | 10 | 10.30 | 0.134 | 0.010 | 16 | 11 |
| 5 | 9.06 | 0.136 | 0.011 | 16 | 10 | 9.62 | 0.137 | 0.012 | 16 | 10 |
| 6 | 9.16 | 0.135 | 0.011 | 4 | 10 | 9.97 | 0.132 | 0.011 | 16 | 11 |
| 7 | 9.24 | 0.136 | 0.010 | 16 | 11 | 9.78 | 0.133 | 0.010 | 16 | 11 |
| 8 | 9.57 | 0.133 | 0.011 | 16 | 10 | 10.04 | 0.136 | 0.010 | 16 | 11 |
| 9 | 9.23 | 0.138 | 0.010 | 16 | 10 | 9.78 | 0.140 | 0.011 | 16 | 10 |
| 10 | 9.41 | 0.135 | 0.011 | 16 | 10 | 10.03 | 0.138 | 0.010 | 16 | 16 |
| 11 | 9.34 | 0.134 | 0.011 | 16 | 10 | 9.74 | 0.137 | 0.010 | 16 | 10 |
| 12 | 9.29 | 0.135 | 0.011 | 4 | 10 | 9.99 | 0.132 | 0.010 | 16 | 10 |
| 13 | 9.15 | 0.131 | 0.011 | 16 | 10 | 9.71 | 0.141 | 0.010 | 16 | 11 |
| 14 | 9.58 | 0.134 | 0.010 | 16 | 11 | 10.11 | 0.136 | 0.010 | 16 | 11 |

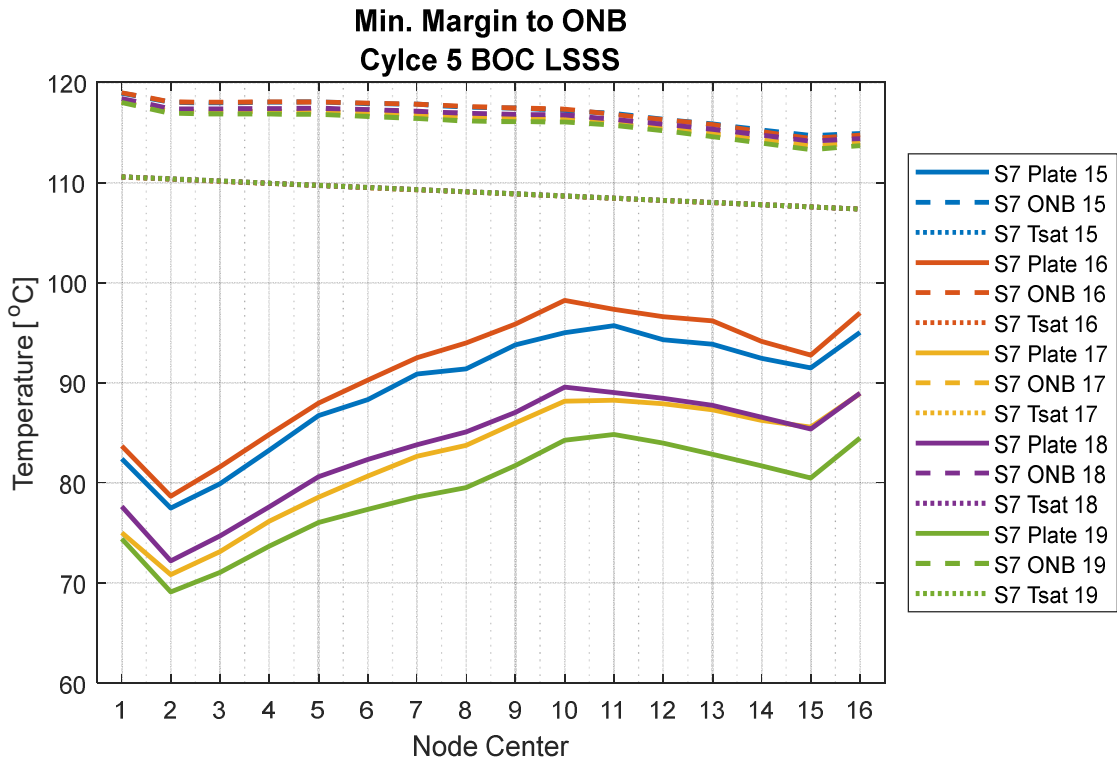


Fig. 9. Cladding outer temperature for Cycle 5 BOC. The saturation and ONB temperatures are also presented.

The nominal cladding outer temperatures for this location are presented in Figure 9, alongside the saturation and ONB temperatures. A minimum margin to ONB of approximately 15 K is maintained during the nominal operation of the reactor.

4. Conclusions

This paper presents the development of a fuel management strategy, which eventually leads to the transition core plan for the MITR LEU conversion. The plan is expected to be included as an appendix chapter in the final SAR. The converted LEU core will start from 22 all fresh LEU fuel elements and gradually transit to a 24-element equilibrium configuration. A routine fuel management with fixed refueling pattern is adopted for the transition period as well as for the equilibrium state.

The results indicate a minimum shutdown margin of 1.42% $\Delta k/k$ during the transition period (comparing to the limit of 1% $\Delta k/k$). The results also confirm that the equilibrium state, where both the shim bank movement (i.e., core reactivity) and the fissile material mass stabilize, can be achieved by applying the analyzed fixed-pattern fuel element reshuffling scheme. Fission density has been evaluated for a number of fully discharged LEU fuel elements, using both conservative and best-estimate approaches. There are adequate margins to the planned qualification fission density limit of three different MITR U-10Mo plate types. The fuel cycle calculations also generate power profiles at each core state. A steady-state thermal-hydraulic safety analysis has been performed, where ONB is considered as the safety criterion. Statistical approach has been adopted for determining the margin to the LSSS power. The results confirm significant margins (more than 2 MW from the licensed power level of 7 MW, i.e., more than 28%) to ONB occurring probability of less than 0.15% (i.e., 3σ) at all analyzed transition and equilibrium fuel cycle states.

Acknowledgements

This research is sponsored by the U.S. Department of Energy, National Nuclear Security Administration Office of Material Management and Minimization Reactor Conversion Program.

References

1. MITR-Staff, Safety Analysis Report for the MIT Research Reactor, MIT-NRL-11-01, 2011, MIT Nuclear Reactor Laboratory.
2. T.H. Newton, Jr., Development of a Low Enrichment Uranium Core for the MIT Reactor, PhD Thesis, 2006, Massachusetts Institute of Technology.

3. A. Bergeron, et al., Low-enriched uranium core design for the Massachusetts Institute of Technology Reactor (MITR) with un-finned 12 mil-thick clad UMo monolithic fuel, ANL/GTRI/TM-13/15, Argonne National Laboratory, Nov. 2013.
4. K. Sun, D. Carpenter, T. Newton, L. Hu, E. Wilson. Evaluation of LEU conversion impact on the in-core experiment performance at the MIT Research Reactor. MIT-NRL-14-02, Rev.1, Feb. 2014.
5. K. Sun, L. Hu, E. Wilson A. Bergeron, T. Heltemes. Low Enriched Uranium (LEU) Conversion Preliminary Safety Analysis Report for the MIT Research Reactor (MITR). MIT-NRL-17-04, Dec. 2017.
6. M. Meyer, et al., Preliminary Report on U-Mo Monolithic Fuel for Research Reactors, INL/EXT-17-40975, Rev. 0, Idaho National Laboratory, Sep. 2017.
7. R. Whittle and R. Forgan, A Correlation for the Minima in the Pressure Drop Versus Flow Rate Curves for Sub-Cooled Water Flowing in Narrow Heated Channel, Nuclear Engineering and Design, Vol. 6, 1967.
8. Y. Sudo, et al., "Experimental Study of Incipient Nucleate Boiling in Narrow Vertical Rectangular Channel Simulating Subchannel of Upgraded JRR-3", J. of Nuclear Science and Technology, 23[1], Jan. 1986.
9. Z. Xu, et al., MCODE, version 2.2 – An MCNP-ORIGEN DEpletion program, Massachusetts Institute of Technology, Feb. 2006.
10. X-5 Monte Carlo Team, MCNP – A general monte carlo N-particle transport code, version 5, LA-UR-03-1987, Los Alamos National Laboratory, Feb. 2008.
11. A. Croff, ORIGEN-2 – A revised and updated version of the Oak Ridge Isotope Generation and Depletion Code, ORNL-5621, Oak Ridge National Laboratory, 1980.
12. Romano, P., Developing Fuel Management Capabilities based on Coupled Monte Carlo Depletion in Support of the MIT Research Reactor Conversion, Master Thesis, 2007, Massachusetts Institute of Technology.
13. Horelik, N., Expanding and Optimizing Fuel Management and Data Analysis Capabilities of MCODE-FM in Support of MIT Research Reactor LEU Conversion, Master Thesis, 2009, Massachusetts Institute of Technology.
14. K. Sun, M. Ames, T. Newton, L. Hu. Validation of a fuel management code MCODE-FM against fission product poisoning and flux wire measurement of the MIT Reactor. Progress in Nuclear Energy, vol. 75: pp. 42-48, 2014.
15. K. Sun, Y. Zeng, T. Newton, L. Hu, A. Bergeron, F. Dunn, and E. Wilson, Neutronic and Thermal-Hydraulic Analyses for Conversion of the MIT Research Reactor (MITR) from Highly Enriched Uranium to Low Enriched Uranium using an Unfinned Fuel Element, MIT-NRL-16-01, Rev.1, May 2016.
16. Relap5/mod3.3 code manual, NUREG/CR-5535/Rev P3, Information Systems Laboratories Inc., Mar. 2003.
17. F. Dunn, L. Hu, and E. Wilson. The STAT7 Code for Statistical Propagation of Uncertainties in Steady-State Thermal Hydraulics Analysis of Plate-Fueled Reactors, ANL/RTR/TM-16/7, Argonne National Laboratory, Dec. 2016.

18. K. Sun, Memo for excel spreadsheets dedicated to MITR fuel management, File Memo, Oct. 2013, MIT Nuclear Reactor Laboratory.